Optics Letters

Numerical algorithm with fourth-order accuracy for the direct Zakharov-Shabat problem

Sergey Medvedev,[1,2,*] Irina Vaseva,[1] Igor Chekhovskoy,[1,2] and Mikhail Fedoruk[1,2]

[1]Institute of Computational Technologies, SB RAS, Novosibirsk 630090, Russia
[2]Novosibirsk State University, Novosibirsk 630090, Russia
*Corresponding author: medvedev@ict.nsc.ru

Received 25 February 2019; revised 26 March 2019; accepted 1 April 2019; posted 3 April 2019 (Doc. ID 360847); published 24 April 2019

We propose a finite-difference algorithm for solving the initial problem for the Zakharov-Shabat system. This method has the fourth order of accuracy and represents a generalization of the second-order Boffetta-Osborne scheme. Our method permits the Zakharov-Shabat spectral problem to be solved more effectively for continuous and discrete spectra.

https://doi.org/10.1364/OL.44.002264

The solution of the direct problem for the Zakharov-Shabat problem (ZSP) is the first step in the inverse scattering transform (IST) for solving the nonlinear Schrödinger equation (NLSE) [1]. The numerical implementation of the IST has gained great importance and attracted special attention since Hasegawa and Tappert [2] proposed to use soliton solutions as a bit of information for fiber optic data transmission.

The direct scattering problem for the NLSE is gaining growing attention in the field of NFT-based telecommunications [3] and various applications of fiber optics [4], such as spectral data search. To calculate such data, it is necessary to solve the initial value problem with respect to the time variable for the Zakharov-Shabat system. Therefore, a lot of effort was made to find effective numerical methods to solve this problem. An overview of the methods used can be found in [3,5,6]. Currently, one of the most effective methods for solving the ZSP is the Boffetta-Osborne (BO) method [7], which has the second order of approximation in the time variable. Comparisons for this method with different other methods were carried out in [6,8].

Beside the approximation accuracy, it is necessary to have an algorithm which has a minimal computational time to get a discrete set of spectral parameters with sufficient accuracy. This approach is implemented in the fast algorithm (FNFT) for solving the direct ZSP using the modified Ablowitz-Ladik method, the Crank-Nicolson scheme [3,9], multistep backward differentiation formula (BDF) and multistep implicit Adams methods [10]. The BO method does not allow a direct application of the fast algorithm, but the fast method can be applied to the split form of the BO method transition matrix [11]. In this Letter, we will focus on building the method of the fourth order of accuracy on a uniform grid. For a non-uniform grid, a fourth-order scheme [12] was applied in [13]. In perspective, the exponential approximation can be applied to our scheme; therefore, we can use the fast algorithm.

We write the Zakharov-Shabat system in a matrix form

$$\frac{d}{dt}\Psi(t) = Q(t)\Psi(t), \tag{1}$$

where $\Psi(t)$ is a complex vector function of the real argument t, $Q(t)$ is a complex matrix

$$\Psi(t) = \begin{pmatrix} \psi_1(t) \\ \psi_2(t) \end{pmatrix}, \qquad Q(t) = \begin{pmatrix} -i\zeta & q(t,z_0) \\ -\sigma q^*(t,z_0) & i\zeta \end{pmatrix},$$

where $q = q(t,z)$ is a complex-valued optical field governing by the NLSE

$$iq_z = \frac{\sigma}{2}q_{tt} + |q|^2 q,$$

$\sigma = \pm 1$ for anomalous and normal dispersion, z_0 plays the role of a parameter and will not be used further. The asterisk means the complex conjugation.

Consider the Jost initial conditions

$$\begin{pmatrix} \psi_1 \\ \psi_2 \end{pmatrix} = \begin{pmatrix} e^{-i\zeta t} \\ 0 \end{pmatrix}[1 + o(1)], \qquad t \to -\infty, \tag{2}$$

which define the Jost solutions for real $\zeta = \xi$. The Jost scattering coefficients $a(\xi)$ and $b(\xi)$ are obtained as limits

$$a(\xi) = \lim_{t\to\infty}\psi_1(t,\xi)e^{i\xi t}, \qquad b(\xi) = \lim_{t\to\infty}\psi_2(t,\xi)e^{-i\xi t}. \tag{3}$$

The function $a(\xi)$ can be extended to the upper half-plane $\xi \to \zeta$, where ζ is a complex number with the positive imaginary part $\eta = \operatorname{Im}\zeta > 0$. The spectral data are determined by $a(\zeta)$ and $b(\zeta)$ in the following way:

(1) the zeros of $a(\zeta) = 0$ define the discrete spectrum $\{\zeta_k\}$, $k = 1, \ldots, K$ of ZSP (1) and phase coefficients

$$r_k = \left.\frac{b(\zeta)}{a'(\zeta)}\right|_{\zeta=\zeta_k}, \qquad \text{where } a'(\zeta) = \frac{da(\zeta)}{d\zeta};$$

(2) the continuous spectrum is determined by the reflection coefficient

$$r(\xi) = \frac{b(\xi)}{a(\xi)}, \qquad \xi \in \mathbb{R}.$$

The matrix $Q(t)$ in the system (1) becomes the skew-Hermitian ($Q^* = -Q^T$) when the spectral parameter $\zeta = \xi$

is real and $\sigma = 1$. Therefore, the system (1) preserves the integral

$$\frac{d}{dt}(|\psi_1(t)|^2 + |\psi_2(t)|^2) = 0. \tag{4}$$

Taking into account the boundary conditions (2), we have

$$|\psi_1(t)|^2 + |\psi_2(t)|^2 = 1. \tag{5}$$

In addition, the trace formula is valid [14]

$$C_n = -\frac{1}{\pi}\int_{-\infty}^{\infty}(2i\xi)^n \ln|a(\xi)|^2 d\xi + \sum_{k=1}^{K}\frac{1}{(n+1)}[(2i\zeta_k^*)^{n+1} - (2i\zeta_k)^{n+1}], \tag{6}$$

which connects the NLSE integrals C_n with the coefficient $a(\xi)$ and the discrete spectrum ζ_k. This formula with $n = 0$ is called the Parseval nonlinear equality and is used to verify the numerical calculations and the consistency of the continuous and discrete spectra found.

We solve the system (1). The matrix $Q(t)$ linearly depends on the complex function $q(t)$, which is given in the whole nodes of the uniform grid $t_n = -L + \tau n$ with a step τ on the interval $[-L, L]$. If the total number of points is $2M + 1$, then the grid step is $\tau = L/M$. Since the matrix $Q(t)$ is specified only on the grid, Boffetta and Osborne suggested replacing the original system on the interval $[t_n - \frac{\tau}{2}, t_n + \frac{\tau}{2}]$ with an approximate system with constant coefficients [7]

$$\frac{d}{dt}\Psi(t) = Q(t_n)\Psi(t), \qquad Q_n = Q(t_n), \tag{7}$$

which is easily solved on the selected interval and gives the transition operator T_n from the layer $n - \frac{1}{2}$ to the layer $n + \frac{1}{2}$:

$$\Psi_{n+\frac{1}{2}} = T_n\Psi_{n-\frac{1}{2}}, \qquad T_n = e^{\tau Q_n}. \tag{8}$$

This method has proven itself well, but nonetheless it might be useful to get a more accurate solution. Hence, we should formulate our task as: it is required to build the transition matrix from $\Psi_{n-\frac{1}{2}}$ to $\Psi_{n+\frac{1}{2}}$ on the interval $[t_n - \frac{\tau}{2}, t_n + \frac{\tau}{2}]$ with highest accuracy possible and minimal computational costs.

The first step towards our goal is a change of variables $\Psi(t) = e^{tQ_n}Y(t)$, so the initial system takes the form

$$\frac{d}{dt}Y(t) = L(t)Y(t), \qquad L(t) = e^{-tQ_n}(Q(t) - Q_n)e^{tQ_n}. \tag{9}$$

In this form, the linear matrix $L(t)$ becomes zero at $t = t_n$, and the derivative of $Y(t)$ is zero at this point. This means that the solution is almost constant in the neighborhood of t_n. If the original system is replaced by

$$\frac{d}{dt}Y(t) = 0, \tag{10}$$

then the transition from $Y_{n-\frac{1}{2}}$ to $Y_{n+\frac{1}{2}}$ becomes trivial:

$$Y_{n+\frac{1}{2}} = Y_{n-\frac{1}{2}}. \tag{11}$$

Returning to the original values of the variable Ψ at the points $t_n - \frac{\tau}{2}$ and $t_n + \frac{\tau}{2}$, we get

$$\Psi_{n-\frac{1}{2}} = e^{(t_n-\frac{\tau}{2})Q_n}Y_{n-\frac{1}{2}}, \qquad \Psi_{n+\frac{1}{2}} = e^{(t_n+\frac{\tau}{2})Q_n}Y_{n+\frac{1}{2}}, \tag{12}$$

which, with regards to solution (11), exactly gives a transition in the BO scheme (8). Since we are interested in the values for Y only in the grid nodes, the solution (11) can be interpreted as a solution to the difference equation

$$\frac{Y_{n+\frac{1}{2}} - Y_{n-\frac{1}{2}}}{\tau} = L_n\frac{Y_{n+\frac{1}{2}} + Y_{n-\frac{1}{2}}}{2}, \tag{13}$$

which is an approximation of the continuous Eq. (9) given that $L_n = L(t_n) = 0$. By decomposing Eq. (13) into a Taylor series at the point $t = t_n$, we obtain the second order of approximation

$$\frac{d}{dt}Y(t_n) - L(t_n)Y(t_n) \approx \frac{\tau^2}{24}\frac{d^3}{dt^3}Y(t_n).$$

Thus, we have shown that the BO scheme corresponds to the simplest finite-difference approximation (13).

There are two possibilities to construct more complex approximations for the Eq. (9) on the interval $[t_n - \frac{\tau}{2}, t_n + \frac{\tau}{2}]$. The first is to build a finite difference analog for this equation. The second possibility is to construct an approximation of the operator $L(t)$ on the entire interval $[t_n - \frac{\tau}{2}, t_n + \frac{\tau}{2}]$ according to the existing values of Q_n on a regular grid and the subsequent solution of such system by any analytical method.

Consider the first approach. As we want to refine the BO scheme, we take the function Y only in two nodes of the grid $Y_{n-\frac{1}{2}}$ and $Y_{n+\frac{1}{2}}$. For the matrix L, we take the three nearest values L_{n-1}, L_n and L_{n+1}. Using these values, we will look for a scheme using the method of uncertain coefficients

$$\frac{Y_{n+\frac{1}{2}} - Y_{n-\frac{1}{2}}}{\tau} = (\alpha L_{n+1} + \beta L_{n-1})Y_{n+\frac{1}{2}} + (\gamma L_{n+1} + \delta L_{n-1})Y_{n-\frac{1}{2}}. \tag{14}$$

Here we used the condition $L_n = 0$, to drop the terms with L_n in the right-hand side. By decomposing expression (14) into a Taylor series at the point $t = t_n$, and using the Eq. (9) at this point and its time derivatives, we found that the expression (14) has at least the fourth-order approximation in τ:

$$\frac{d}{dt}Y(t_n) - L(t_n)Y(t_n) \approx \frac{\tau^4}{24}(\beta - \alpha)\frac{dL_n}{dt}\frac{d^2L_n}{dt^2}Y_n - \frac{\tau^4}{5760}\left(17\frac{d^4L_n}{dt^4} + 12\frac{d^2L_n}{dt^2}\frac{dL_n}{dt}\right)Y_n$$

for $\gamma = 1/24 - \alpha$, $\delta = 1/24 - \beta$ and arbitrary α and β. The resulting scheme can be rewritten as

$$[I - \tau\alpha L_{n+1} - \tau\beta L_{n-1}]Y_{n+\frac{1}{2}} = \left[I + \tau\left(\frac{1}{24} - \alpha\right)L_{n+1} + \tau\left(\frac{1}{24} - \beta\right)L_{n-1}\right]Y_{n-\frac{1}{2}}, \tag{15}$$

where

$$L_{n+1} = e^{-(t_n+\tau)Q_n}(Q_{n+1} - Q_n)e^{(t_n+\tau)Q_n},$$
$$L_{n-1} = e^{-(t_n-\tau)Q_n}(Q_{n-1} - Q_n)e^{(t_n-\tau)Q_n}.$$

In the original variables, this scheme will take the following form

$$[I - \tau\alpha M_{n+1} - \tau\beta M_{n-1}]e^{-\frac{\tau}{2}Q_n}\Psi_{n+\frac{1}{2}} = \left[I + \tau\left(\frac{1}{24} - \alpha\right)M_{n+1} + \tau\left(\frac{1}{24} - \beta\right)M_{n-1}\right]e^{\frac{\tau}{2}Q_n}\Psi_{n-\frac{1}{2}}, \tag{16}$$

where

$$M_{n+1} = e^{-\tau Q_n}(Q_{n+1} - Q_n)e^{\tau Q_n},$$
$$M_{n-1} = e^{\tau Q_n}(Q_{n-1} - Q_n)e^{-\tau Q_n}.$$

For real values $\zeta = \xi$, energy conservation [Eq. (5)] is important, so if $\alpha = \beta = 1/48$, then the transition operator

$$T_n = e^{\frac{\xi}{2}Q_n}\left[I - \frac{\tau}{48}(M_{n+1} + M_{n-1})\right]^{-1} \times \left[I + \frac{\tau}{48}(M_{n+1} + M_{n-1})\right]e^{\frac{\xi}{2}Q_n} \quad (17)$$

becomes a unitary matrix that conserves quadratic energy [Eq. (5)]. Indeed, the spectrum of matrices Q_n is purely imaginary; therefore, the exponent $e^{\frac{\xi}{2}Q_n}$ is unitary. The expression with square brackets is the Cayley transform of the skew-Hermitian matrix $\frac{\tau}{48}(M_{n+1} + M_{n-1})$ into a unitary one. The transmission matrix (17) was obtained using a transformation of variables, and it conserves the energy for the real spectral parameters; therefore, the corresponding scheme will be called as the fourth-order conservative transformed scheme (CT4).

The spectral parameter ξ is included only through exponents, as in the BO method; therefore, the use of the fast algorithm (FNFT) is difficult [9], but it is possible after exponential approximation [11]. Due to the presence of an inverse matrix in the transition operator, the fast calculation scheme can be constructed similarly to the approach for the Crank-Nicolson scheme [9]: we have to replace the transition operator with the ratio of the matrix polynomial to the linear polynomial. The complete formulas for calculating are rather cumbersome; therefore, they are not given in this Letter.

An open question is how to use free parameters a and b for computation with complex spectral parameters. Although the preservation of high-frequency oscillations is important, for the eigenvalues near the imaginary axis, another criterion for the scheme may be needed.

The following formula was used to calculate the approximation order m:

$$m = \log_{\frac{\tau_1}{\tau_2}} \frac{\|\tilde{\Psi}_1(L)\|_2}{\|\tilde{\Psi}_2(L)\|_2} = \frac{\log_2 \frac{\|\tilde{\Psi}_1(L)\|_2}{\|\tilde{\Psi}_2(L)\|_2}}{\log_2 \frac{\tau_1}{\tau_2}}, \quad (18)$$

where τ_i, $i = 1$, and 2 are the steps of computational grids for two calculations with one spectral parameter ζ and $\tau_1 > \tau_2$, $\tilde{\Psi}_i(L)$ is a deviation of the calculated value $\Psi_i(L)$ from the exact analytical value $\tilde{\Psi}_i(L)$ at the boundary point $t = L$. The calculations were carried out for different p-norms and showed close values for the approximation orders. However, for the Euclidean 2-norm, the graphs were the smoothest.

The scheme (17) was tested for different model signals, where the analytical expressions for spectral data were known. In particular, various calculations exist for the oversoliton from [15] for a small number of discrete eigenvalues. However, to present our scheme (17), we chose calculations for one soliton potential $q(t) = \mathrm{sech}(t)$ because this solution is smooth and not only spectral data are known for it but also eigenfunctions [16]. It has a single eigenvalue $\zeta_1 = 0.5i$, $b(\zeta_1) = -1$. Since this potential is purely solitonic $b(\xi) = 0$, the continuous spectrum energy $E_c = -\frac{1}{\pi}\int_{-\infty}^{\infty} \ln|a(\xi)|^2 d\xi = 0$, while $a(\xi) = (\xi - 0.5i)/(\xi + 0.5i)$. Here we present the comparison of BO, CT4, and Runge-Kutta fourth-order algorithm (RK4) [8].

Figure 1 demonstrates the approximation order m of three schemes with respect to a spectral parameter $\xi \in [-20, 20]$. Each line was calculated by the formula (18) using two embedded grids with a doubled grid step $\tau = L/M$, $L = 40$, where coarse and fine grids were defined by $M = 2^{10}$ and 2^{11}. Note also that the approximation order holds for discrete eigenvalues.

Figures 2 and 4 present the errors calculated using the BO, CT4, and RK4 schemes. If $\delta_\phi = \phi^{\text{computed}} - \phi^{\text{exact}}$ (ϕ can be a or b) then $\text{error}[\phi(\zeta)] = \sqrt{\text{Re}[\delta_\phi(\zeta)]^2 + \text{Im}[\delta_\phi(\zeta)]^2}$. Since the exact values of $|a|$, $|b|$ are either 0 or 1, we use the absolute error here.

Figure 2 shows the continuous spectrum errors for the fixed value of the spectral parameter $\xi = 20$. The vertical line in Fig. 2 marks the minimum number of grid nodes $M_{\min}$ that guarantee a good approximation. Actually, when the continuous spectrum is calculated, it is necessary to choose a time step $\tau = L/M$ to describe the fastest oscillations correctly. For a fixed value of ξ, the local frequency $\omega(t;\xi) = \sqrt{\xi^2 + |q(t)|^2}$ of the system (1) varies from $\omega_{\min} = |\xi|$ to $\omega_{\max} = \sqrt{\xi^2 + q_{\max}^2}$, where $q_{\max} = \max_t|q(t)|$ is the maximum absolute value of the potential $q(t)$. Therefore, step τ cannot be arbitrary. In order to describe the most rapid oscillations, it is necessary to have at least 4-time steps for the oscillation period, so the inequality must be satisfied: $4\tau = 4L/M \le 2\pi/\omega_{\max}$. Therefore, any difference schemes will

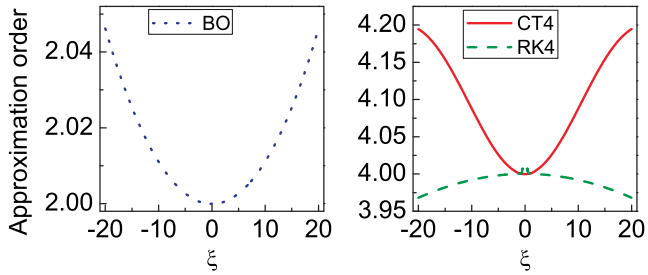

Fig. 1. Approximation order of the Boffetta-Osborne (BO), conservative transformed (CT4), and Runge-Kutta fourth-order (RK4) schemes.

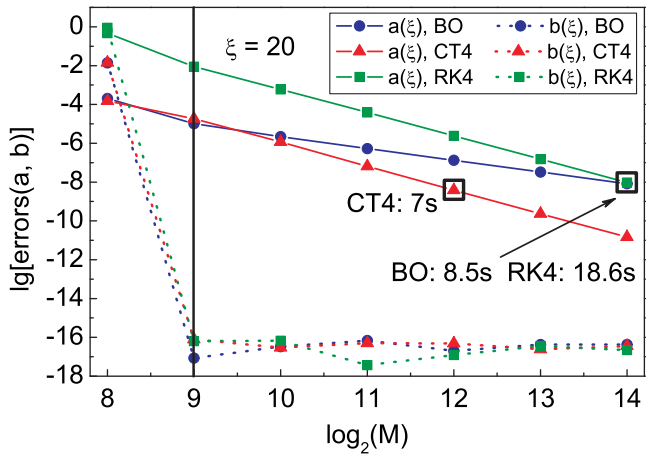

Fig. 2. Continuous spectrum errors.

approximate the solutions of the original continuous system (1) if the inequality is fulfilled for the number of points $M \geq M_{\min} = 2L\omega_{\max}/\pi$.

The continuous spectrum energy computed by three schemes is presented in Fig. 3. It is important to define the size of the spectral domain L_ξ and the corresponding grid step $d\xi$ for the calculation of the continuous spectrum energy. According to the conventional discrete Fourier transform, we take the same number of points $N_\xi = N$ in the spectral domain and define a spectral step as $d\xi = \pi/(2L)$. Thus, the size of the spectral interval is $L_\xi = \pi/(2\tau)$. The energy integral was computed by the trapezoid rule. When the truncation error becomes small, the round-off error dominates. Any further decrease of a step size leads to the total computational error increasing. This effect can be observed for CT4 graph in Fig. 3.

The discrete spectrum errors are presented in Fig. 4. The parameters $a(\zeta)$ and $b(\zeta)$ were computed for the analytically known eigenvalue $\zeta_1 = 0.5i$. In this test, we did not use any numerical algorithm to find the eigenvalue but compute $a(\zeta)$ and $b(\zeta)$ at the exact point $\zeta = \zeta_1$ right away. It was made intentionally to estimate the error of the scheme itself and avoid the influence of other numerical algorithm errors. It should be noted that the parameter $b(\zeta)$ can be computed straightforwardly for these type of potentials, but in the case of multiple solitons, one should use different special techniques [17,18].

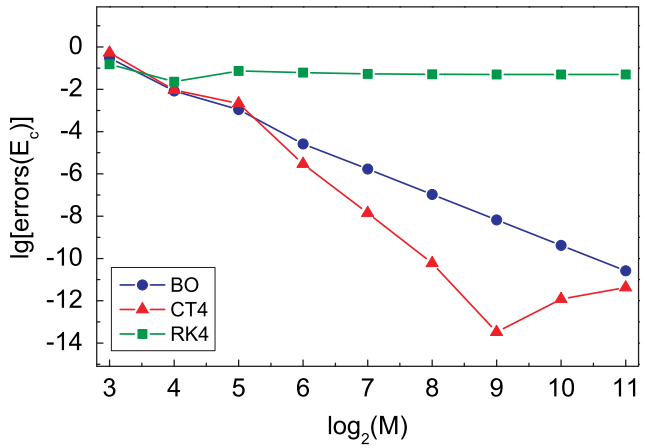

Fig. 3. Continuous spectrum energy, $E_c^{\text{exact}} = 0$.

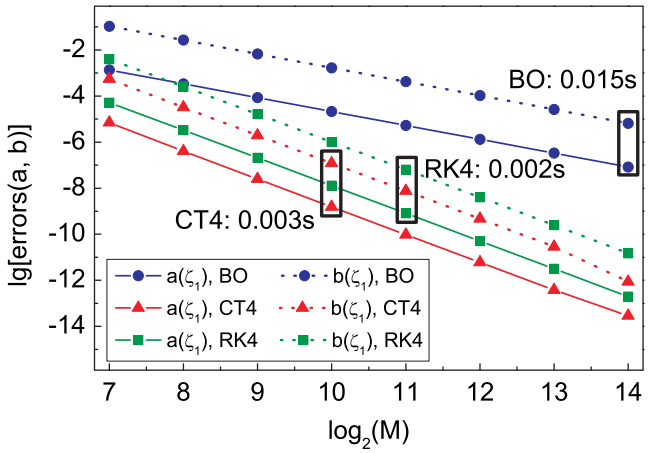

Fig. 4. Discrete spectrum errors.

Figures 2 and 4 also demonstrate a comparison of the computational time. It is shown that CT4 scheme allows achieving better accuracy faster than the BO scheme. RK4 scheme gives the same result as CT4 for discrete spectrum, but it functions worse when it comes to the continuous spectrum with large values of ξ. The reason for this is the fact that RK4 scheme does on conserve the continuous spectrum energy, which is confirmed by the Fig. 3.

In this Letter, we proposed the family of fourth-order finite-difference one-step schemes to solve the direct Zakharov-Shabat problem on a uniform grid. Among this family, a quadratic integral preserving scheme for the continuous spectrum was distinguished. Numerical experiments for the soliton potential confirmed the theoretical order of approximation and demonstrated a significant advantage of our conservative scheme over the Boffetta-Osborne scheme. The proposed scheme works for uniform grids, which can be useful when processing optical signals recorded at the receiver at regular time intervals. The high efficiency of our scheme can improve the performance of recently proposed soliton search methods such as, for example, the contour integral approach [19] if our scheme is used for computing contour integrals and the iterative gradient descent algorithm approach [20] if the continuous spectrum is computed by our scheme.

Funding. Russian Science Foundation (RSF) (17-72-30006).

REFERENCES

1. V. E. Zakharov and A. B. Shabat, J. Exp. Theor. Phys. **34**, 62 (1972).
2. A. Hasegawa and F. Tappert, Appl. Phys. Lett. **23**, 142 (1973).
3. S. K. Turitsyn, J. E. Prilepsky, S. T. Le, S. Wahls, L. L. Frumin, M. Kamalian, and S. A. Derevyanko, Optica **4**, 307 (2017).
4. F. Braud, M. Conforti, A. Cassez, A. Mussot, and A. Kudlinski, Opt. Lett. **41**, 1412 (2016).
5. M. I. Yousefi and F. R. Kschischang, IEEE Trans. Inf. Theory **60**, 4329 (2014).
6. A. Vasylchenkova, J. Prilepsky, D. Shepelsky, and A. Chattopadhyay, Commun. Nonlinear Sci. Numer. Simul. **68**, 347 (2019).
7. G. Boffetta and A. Osborne, J. Comput. Phys. **102**, 252 (1992).
8. S. Burtsev, R. Camassa, and I. Timofeyev, J. Comput. Phys. **147**, 166 (1998).
9. S. Wahls and H. V. Poor, in *IEEE International Conference on Acoustics, Speech and Signal Processing* (IEEE, 2013), pp. 5780–5784.
10. V. Vaibhav, IEEE Photon. Technol. Lett. **30**, 700 (2018).
11. P. J. Prins and S. Wahls, in *ICASSP, IEEE International Conference on Acoustics, Speech and Signal Processing—Proceedings* (IEEE, 2018), Vol. **4**, pp. 4524–4528.
12. S. Blanes, F. Casas, and M. Thalhammer, Comput. Phys. Commun. **220**, 243 (2017).
13. S. Chimmalgi, P. J. Prins, and S. Wahls, "Fast nonlinear Fourier transform algorithms using higher order exponential integrators," arXiv:1812.00703 (2018).
14. M. J. Ablowitz and H. Segur, *Solitons and the Inverse Scattering Transform* (Society for Industrial and Applied Mathematics, 1981).
15. J. Satsuma and N. Yajima, Progr. Theoret. Phys. Suppl. **55**, 284 (1974).
16. A. Hasegawa and Y. Kodama, *Solitons in Optical Communications* (Clarendon; Oxford University, 1995).
17. S. Hari and F. R. Kschischang, J. Lightwave Technol. **34**, 3529 (2016).
18. V. Aref, "Control and detection of discrete spectral amplitudes in nonlinear Fourier spectrum," arXiv:1605.06328 (2016).
19. A. Vasylchenkova, J. E. Prilepsky, and S. K. Turitsyn, Opt. Lett. **43**, 3690 (2018).
20. V. Aref, S. T. Le, and H. Buelow, "An efficient nonlinear Fourier transform algorithm for detection of eigenvalues from continuous spectrum," arXiv:1812.02092 (2018).